analytical chemistry

pubs.acs.org/ac Article

Ensemble Sensing Using Single-Molecule DNA Copolymers

Sagun Jonchhe, Sangeetha Selvam, Deepak Karna, Shankar Mandal, Benjamin Wales-McGrath, and Hanbin Mao*

Cite This: *Anal. Chem.* 2020, 92, 13126–13133 Read Online

ACCESS | Metrics & More | Article Recommendations | Supporting Information

ABSTRACT: While single-molecule sensing has offered ultimate mass sensitivity at the precision of individual molecules, it requires a longer time to detect analytes at lower concentrations when analyte binding to single-molecule probes becomes diffusion-limited. Here, we solved this accuracy problem in the concentration sensitivity determination by using single-molecule DNA homopolymers, in which up to 473 identical sensing elements (DNA hairpins) were introduced by rolling circle amplification. Surprisingly, the DNA homopolymers containing as few as 10 tandem hairpins displayed ensemble unfolding/refolding transitions, which were exploited to recognize microRNAs (miRNAs) that populated unfolded hairpins. Within 20 min, the femtomolar detection limit for miRNAs was observed, 6 orders of magnitude better than standalone hairpins. By incorporating different hairpin probes in an alternating DNA copolymer, multiplex recognition of different miRNAs was demonstrated. These DNA co-polymers represent new materials for innovative sensing strategies that combine the single-molecule precision with the accuracy of ensemble assays to determine concentration sensitivities.

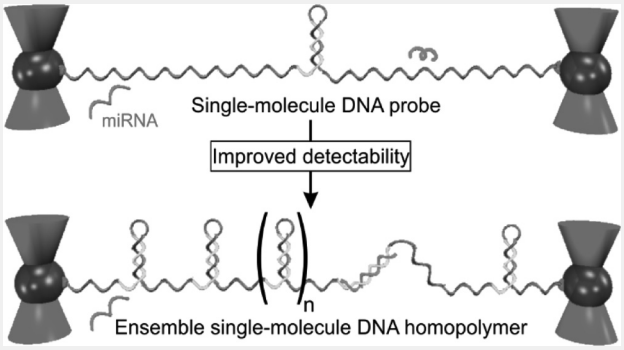

Conventional sensing is usually carried out at the ensemble level where average signals are collected from many indistinguishable probing units. The averaged signal provides high accuracy in the sensing at the expense of molecular precisions. Single-molecule sensing[1−3] offers ultimate mass sensitivity at the precision of individual target molecules, which represents a superior mass detection limit. However, single-molecule sensing often does not have the accuracy to obtain a superlative concentration detection limit in a fixed time. To achieve single-molecule mass sensitivity, a probe, which is often a single molecule by itself, is designed to have a small cross section to interact with individual analyte molecules. The small cross section causes a slow, diffusion-limited process in which a prolonged waiting time is required for single analyte molecules to bind to the probes for detection, thereby compromising the accuracy in the determination of the concentration detection limit. To address this issue, a single-molecule array[2] has been used to substantially expand the sensing area. Because each signal generated from individual probing units in an array is still stochastic in nature, a large array set is required to generate results with accuracy approaching to the ensemble sensing.

Such a strategy, however, raises the question whether probing units in an array have the same behavior as standalone units. It is well known that single molecules display stochastic behaviors drastically different from bulk materials that show ensemble average properties. When the number of the single-molecule units increases, their properties may behave collectively because of indistinguishable fluctuations among individual units. The minimal number of individual units that start to show ensemble properties is not known, which is critical not only to understand the properties and activities of tandemly arranged biomolecules inside cells[4−8] but also to design better single-molecule sensors.

In this work, we first used rolling circle amplification (RCA)[9,10] to prepare DNA homopolymers by introducing tandemly arranged identical DNA structures,[11] such as hairpins, in a single-stranded DNA template. We found that as few as 10 DNA hairpins in a tandem array are sufficient to show ensemble folding and unfolding transitions. Leveraging the ensemble behaviors of these hairpins that bind to microRNA (miRNA) in the single-molecule DNA homopolymer template, we observed the detection of femtomolar miRNA targets within 20 min, which represented a 6-order magnitude improvement in the detection limit with respect to that of standalone hairpin probes. By incorporating two different hairpin probes alternatively arranged in the so-called alternating DNA copolymer, multiplex sensing for different miRNAs has been demonstrated in single-molecule templates.

Received: May 22, 2020
Accepted: August 23, 2020
Published: August 24, 2020

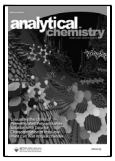

https://dx.doi.org/10.1021/acs.analchem.0c02196
Anal. Chem. 2020, 92, 13126−13133

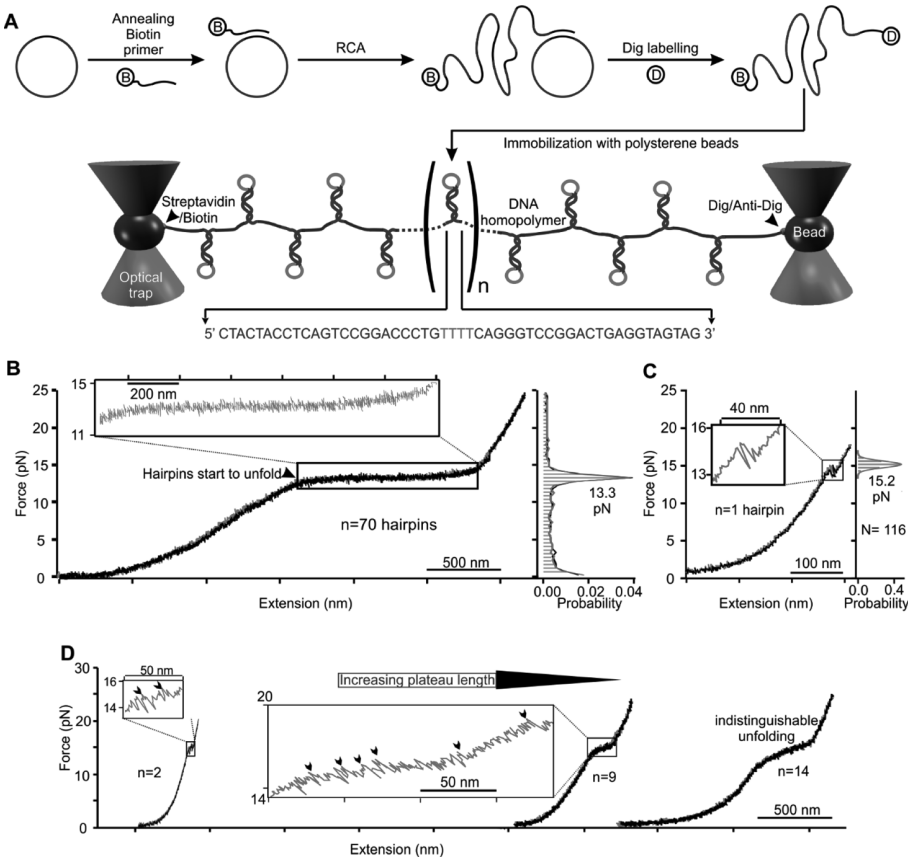

Figure 1. Ensemble unfolding/refolding transitions of tandem DNA hairpins in DNA homopolymers. (A) Rolling cycle amplification to prepare DNA homopolymers with tandem DNA hairpins. (B) Force−extension curves of 70 hairpins in the DNA copolymer show indistinguishable unfolding (red) and refolding (black) of individual hairpins at a plateau centered at 13.3 pN (transition starts at 13.0 pN), which is characteristic of ensemble transitions. Force histogram derived from the unfolding curve is shown to the right. As controls, one (C) and two (D) hairpins tethered between two duplex DNA handles show individual transitions at higher forces (15.2 ± 0.1 and 14.4 ± 0.1 pN for standalone and two-hairpin constructs, respectively; see histograms in (C) and Figure S10; N is the number of features). (D) Individual unfolding (red) and refolding (black) events were observed in $n < 10$ hairpins but not in $n = 14$ hairpins (see Figure S13 for the blowup plateau). Arrowheads depict individual transition events for DNA hairpins.

Because of the high versatility of various DNA recognition elements and their facile preparations in the new DNA copolymer materials, we expect that this ensemble sensing strategy can accurately detect a wide range of different analytes simultaneously with single-molecule precisions.

■ EXPERIMENTAL SECTION

Materials. Unless specified, all the reagents are purchased from VWR (Radnor, PA) with a minimum purity of >99.0%. The DNA oligomers were purchased from Integrated DNA Technology (IDT, Coralville, IA), which were purified with polyacrylamide gel electrophoresis and stored at −20 °C. Purified miRNA oligomers were purchased from IDT, diluted into desired concentrations with 10 mM Tris buffer (pH 7.4), aliquoted, and stored at −80 °C. Streptavidin and digoxigenin (Dig) antibody-coated polystyrene beads were purchased from Spherotech (Lake Forest, IL). XbaI, SacI, EagI and BsaI-HF v2 enzymes were purchased from New England Biolabs (NEB, Ipswich, MA). Digoxigenin dUTP (Dig-dUTP) was purchased from Roche or Enzo Life Science. Terminal transferase and Phi 29 enzymes were obtained from Thermo Fischer (Waltham, MA) and Mclab (South San Francisco, CA), respectively.

Synthesis of the Single-Hairpin Construct. To synthesize the standalone DNA hairpin construct used in Figure 1C, oligo-1 (Table S3) containing a part of the hairpin stem was annealed with oligo-4. The annealed fragment was ligated with the 2028 bp DNA handle (see SI) and gel purified. For the other end of the standalone DNA hairpin construct, oligo-2 containing the other end of the DNA hairpin was annealed with oligo-5. This fragment was then ligated with a 2690 bp DNA handle (see SI) and gel purified. Finally, the standalone DNA construct was synthesized using T4 DNA ligase (NEB) through a three-piece ligation of the purified 2028 bp DNA handle, the 2690 bp DNA handle, and the oligo-3 that contained a tetrathymine (T4) loop. For the standalone DNA construct used in Figure S16, oligo-6 that contained the hairpin (Table S3) was annealed with oligo-7 and oligo-8. The annealed product was ligated with the 2028 bp DNA handle and purified by agarose gel. The purified oligo was then annealed and ligated with the 2391 bp DNA handle (see SI) to get the final product.

Synthesis of the Double-Hairpin Construct. The double-hairpin construct was prepared by the splint ligation. The oligo-9, oligo-10, and oligo-8; and oligo-11, oligo-12, and oligo-7 (Table S3) were annealed and ligated separately to form two hairpins HP1 and HP2 (Figure S1). The HP1 and

https://dx.doi.org/10.1021/acs.analchem.0c02196
Anal. Chem. 2020, 92, 13126−13133

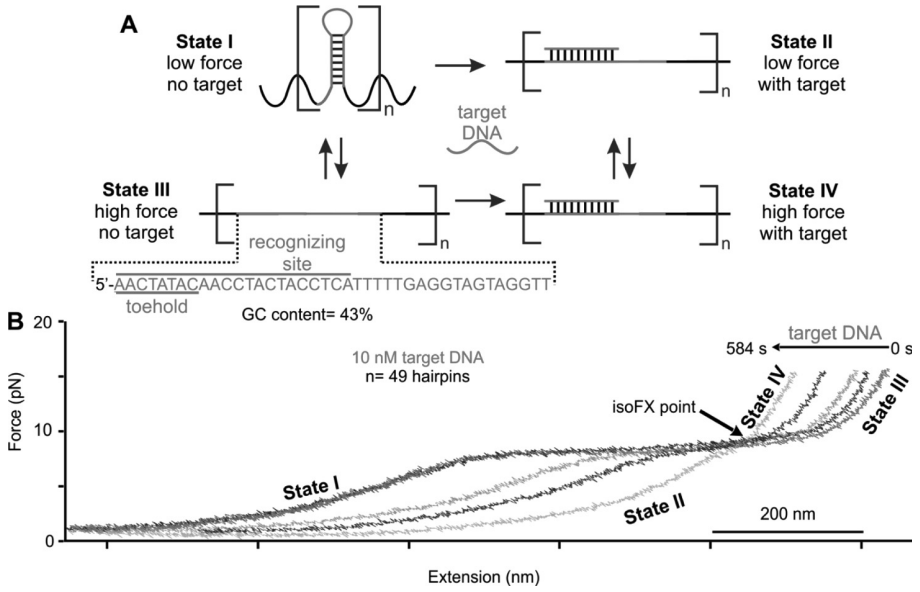

Figure 2. Hybridization between target DNAs and tandem hairpins in DNA homopolymers. (A) Mechanochemical interaction cycle between target DNAs and tandem DNA hairpins. At the force below the transition plateau, the folded hairpin (state I) binds to the target DNA (pink) via the toehold (the green region flanking the hairpin stem), which leads to the chemical unfolding of the hairpin (state II). At the high force above the transition plateau, the hairpin is mechanically unfolded (state III). Binding of the target DNA to state III decreases the extension of the construct (state IV). (B) F−X curves of a 49-hairpin template in 10 nM target DNA during 584 s. See Figures S14 and S15 for FJC and WLC fittings of curves, respectively. All the curves pass through an identical spot named as the isoFX point.

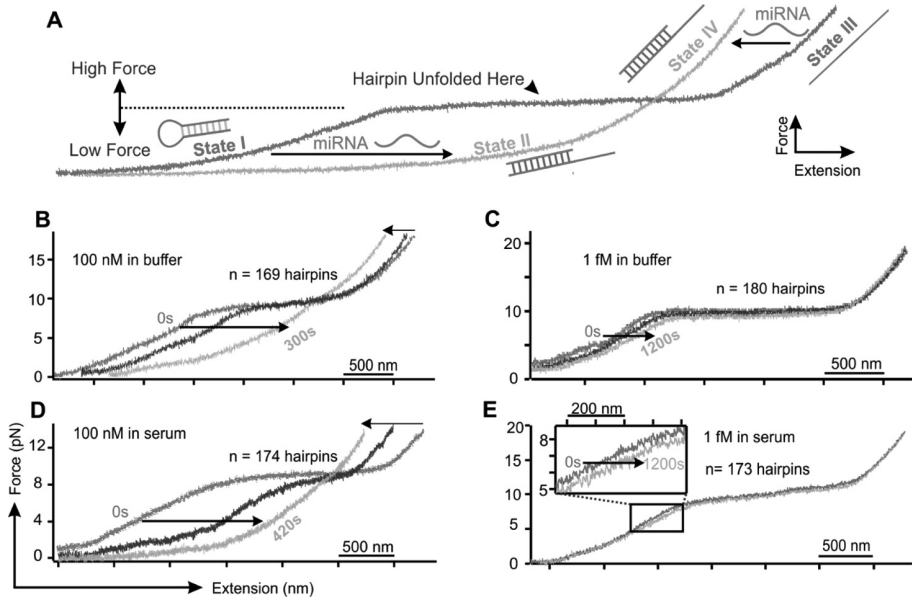

Figure 3. Single-molecule sensing using ensemble behavior of tandem hairpins in DNA homopolymers. (A) Sensing is based on the mechanochemical interaction cycle (see Figure 2A) between tandem hairpins and miRNA Let-7a (pink). F−X curves of the tandem hairpins with and without 100 nM (B, 169 hairpins) and 1 fM (C, 180 hairpins) Let-7a miRNA in a 10 mM Tris buffer supplemented with 100 mM KCl at pH 7.4. F−X curves of the tandem hairpins with and without 100 nM (D, 174 hairpins) and 1 fM (E, 173 hairpins, inset shows an expanded region) Let-7a miRNA in the same Tris buffer supplemented with 10% human serum.

HP2 were annealed and ligated with the 2028 bp DNA handle and the 2391 bp DNA handle, respectively, followed by purification. Purified products were splint-ligated to form a double-hairpin construct by using the splint (oligo-13) and T4 DNA ligase (NEB). The splint was finally removed by supplying an excess of the splint remover (oligo-14). Note that the connecting region between the two hairpins is identical to that between the neighboring hairpins in the RCA construct used in Figure 1.

Syntheses of the DNA Homopolymer and Copolymer Using RCA. The DNA homopolymer and copolymers were prepared via syntheses of circular templates, amplifications using the circular templates, and digoxigenin labeling (Figure S3).[11] The purified 5′ phosphorylated linear templates (oligo-19 for the tandem hairpins used in Figure 1, oligo-20 for the

https://dx.doi.org/10.1021/acs.analchem.0c02196
Anal. Chem. 2020, 92, 13126−13133

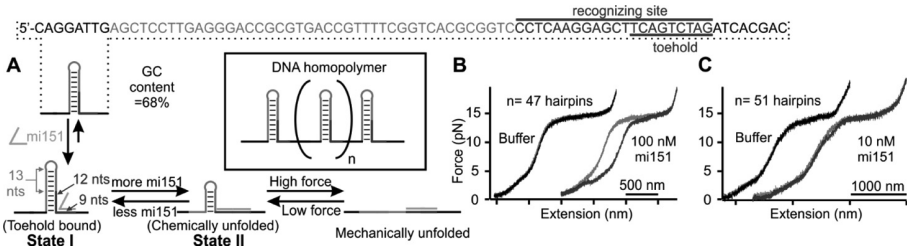

Figure 4. Single-molecule sensing using tandem DNA hairpins with high GC content in a DNA homopolymer. (A) Transition pathway of the DNA homopolymer (inset) upon binding with the mi151 (orange). Sequence for the DNA hairpin is shown at the top. Each hairpin is dispersed with a 25 nt spacer to its neighbor. Underlined and toplined portions indicate the toehold and miRNA recognizing regions, respectively. Stretching (red) and relaxing (black or blue) F−X curves without (left) and with (right) mi151 target in a 10 mM Tris buffer supplemented with 100 mM KCl at pH 7.4 for (B) 100 nM and (C) 10 nM mi151.

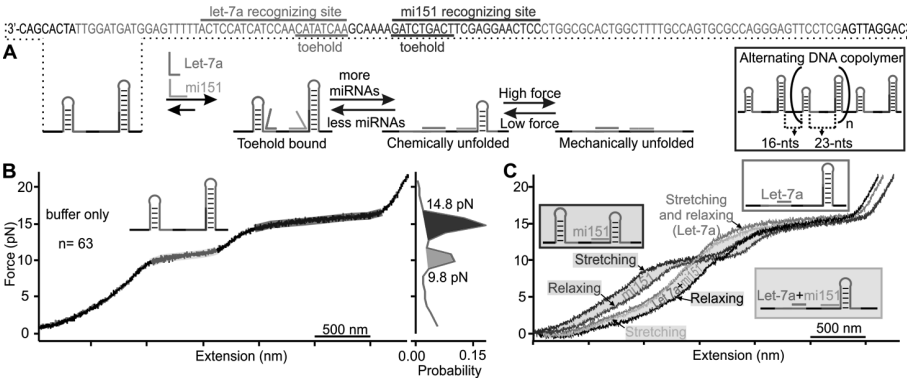

Figure 5. Multiplex sensing using single-molecule alternating DNA copolymers. (A) Transition pathway of the two hairpins upon binding of both Let-7a (pink) and mi151 (orange) miRNA targets. Inset shows the schematic of the alternating DNA copolymer. Sequence for hairpins is shown at the top. Underlined and toplined portions indicate the toehold and miRNA recognizing sites of the hairpins, respectively. 16 and 23 nt spacers are placed between two alternatively arranged hairpins. (B) Stretching (red) and relaxing (black) F−X curves of the alternating DNA copolymer (n = 63 hairpins) in a 10 mM Tris buffer supplemented with 100 mM KCl at pH 7.4. Green and blue colors depict unfolding plateaus for the low (43%) and high (68%) GC content hairpin probes, respectively. The same color code is used to indicate the unfolding plateau force histograms in the right panel. (C) Overlapped F−X curves in the presence of 100 nM Let-7a miRNA (pink), 100 nM mi151 (stretching-blue, and relaxing-dull blue), and both 100 nM Let-7a and 100 nM mi151 (stretching-brown, and relaxing-black). The curves show hystereses in the presence of mi151 (cyan) and both miRNAs (green). Color coded insets indicate schematics of the miRNA-bound hairpin probes.

sensing hairpins shown in Figures 2 and 3, oligo-21 for the sensing hairpins shown in Figure 4, and oligo-22 for the sensing hairpins shown in Figure 5) were annealed and splint ligated using a splint (oligo-14) and T4 DNA ligase (NEB) at 16 °C for 16 h. The splint was removed by a splint remover (oligo-13) which contains a sequence complementary to the splint. The reaction was treated with Exonuclease I and Exonuclease III (NEB) to remove all the linear DNA strands in the reaction. The obtained circular DNA templates were then annealed with the biotinylated primer (5'-Biotin-GCA TTA GGA AGC AGC CCA GTA GTA GGA TCA CGA CCA GGA TTG) (see Figure S2 for the preparation of the biotinylated primer). RCAs were carried out using Phi 29 enzyme (Mclab) at 37 °C for 30 s to 20 min to obtain linear ssDNA homopolymers with different lengths (Figure S4). The resulting DNA homopolymers were labeled with digoxigenin using Dig-dUTP (either from Roche or from Enzo Life Science) and terminal transferase (Thermo Fischer) at 37 °C for 3 h. The constructs were stored in 4 °C and used within a week.

Preparation of Microfluidic Chambers. A four-channel microfluidic chamber was used for single-molecule experiments (Figure S5).[12] The chamber was made by thermal bonding of a parafilm (thickness 0.127 mm, Bemis Co., Neenah, WI) between two pieces of cover glass (#1, VWR, size 24 × 60 mm). The parafilm contained a desired pattern cut by a laser (Versa Laser, Scottsdale, AZ). The top and bottom channels were used to introduce streptavidin-coated and Dig-antibody-coated polystyrene beads, respectively. Two middle channels merged in the midway to form a Y-shaped flow pattern. The two middle channels were connected to the top and bottom channels with micropipettes (Garner Glass Co., i.d. 25 μm). Inlet and outlet holes through one cover glass were drilled by a Versa laser cutter described above. The chamber was fixed in a homemade bracket, which was then fixed in a home-made laser tweezer instrument.[13] Two buffers with different chemical compositions were separately introduced to the two middle channels by a Harvard Apparatus PHD 2000 pump (Harvard Apparatus, South Natick, MA) with a flow rate maintained at 0.2 μL/min.

Mechanical Unfolding Experiments. In the microfluidic flow system, two optical traps in a home-made laser tweezer system[13] were employed to capture two different beads at 25 °C. These two traps (350 mW power for each) were generated by a focusing objective [Nikon CFI-PlanApochromat 60×, numerical aperture (NA) 1.2, water immersion, working distance ∼320 μm] from collimated S- and P-polarized laser beams, which were emitted from a CW diode-pumped solid-state laser (1064 nm, 5W, IPG Photonics). By using a steerable mirror (Nano MTA, Mad City Laboratories, Madison, WI),

https://dx.doi.org/10.1021/acs.analchem.0c02196
Anal. Chem. 2020, 92, 13126−13133

one of the trapped polystyrene beads (1.87 μm diameter), which contained the DNA construct through the biotin/streptavidin interaction, was moved close to the anti-digoxigenin-coated polystyrene bead (2.10 μm diameter) trapped by another laser. By the anti-Dig/Dig interaction, the single-molecule DNA construct was tethered between the two trapped beads. Once a tether was obtained, force ramping at a 5.5 pN/s loading rate (in 10−30 pN range) was carried out to mechanically unfold DNA hairpins in the constructs. The force was recorded in a Labview 8 (National Instruments, Austin, TX) program and treated by Igor programs (Wavemetrics, Portland, OR) to generate force−extension curves. All mechanical unfolding experiments were carried out in 10 mM Tris buffers supplemented with 100 mM KCl (pH 7.4).

■ RESULTS AND DISCUSSION

Ensemble Behaviors of DNA Hairpins in DNA Homopolymers. First, we employed RCA[9,10] to introduce up to 473 DNA hairpins in a DNA homopolymer with 28 nucleotides (nts) spacer between each hairpin (Figures 1A, see S6 for calculation of the number of hairpins). The DNA homopolymer was then labeled with biotin and digoxigenin at two ends separately so that it can be anchored between two optically trapped polystyrene particles (see Supporting Information and Experimental Section). Next, we performed mechanical unfolding and refolding of tandem hairpins with single-molecule force spectroscopy experiments.[14−18] We anticipated multiple sawtooth-like features in force−extension curves that correspond to the unfolding or refolding of many hairpins around 15 pN.[19] Surprisingly, a smooth force plateau was observed instead (Figure 1B). Not only were unfolding and refolding features drastically different from standalone hairpins (Figure 1C), the starting force (see Figure S9) of the plateau was also lower than that for the unfolding of standalone hairpins, suggesting that it is easier to unfold tandem DNA hairpins than standalone units. This can be rationalized by the fact that due to the sphere-like charge distribution in folded hairpins, counter ion condensation does not screen electrostatic interactions[20] as expected in linear polyelectrolytes.[21,22] As a result, the folded structures experience a higher repulsive force originated from the neighboring hairpins that have higher charge densities than single-stranded DNA in the homopolymer. To provide evidence for this charge effect, we added 20 mM Mg^{2+} in the buffer, which is known to shield the charge effect.[23,24] In the presence of Mg^{2+}, we observed that the unfolding plateau force for tandem hairpins was increased (Figure S11), confirming that the charge shielding enhanced the mechanical stability of tandem DNA hairpins in the homopolymer.

The smooth transition plateau at a constant force resembles phase transitions in bulk in which the temperature remains constant until all the molecules convert from one phase to another. Therefore, the transition plateau can be used to indicate the ensemble behavior of tandem hairpins in the DNA homopolymer. It is possible that other structures, such as stem-bulge or long-range hybridization of complementary strands (Figure S12), may form in this RCA construct. To confirm that tandem DNA hairpins are formed, first, we calculated mfold structures. The tandem arrangement is the most thermodynamically stable conformation in the DNA construct that contains 3, 4, or 10 hairpins. Kinetically, the tandem hairpin formation in the DNA homopolymer has the least entropic penalty as a hairpin-stem forming DNA sequence hybridizes with its complementary sequence in proximity, instead of that far away. Second, we prepared an alternating DNA copolymer in which two different hairpins (see Figure 5A,B below) are incorporated alternatively without base-pairing complementarity between their respective stems. If it were true that the stem-bulge conformation or other higher order conformations are responsible for the observed plateau, only one force plateau is expected in the unfolding of this alternating DNA copolymer. However, we observed two distinct transition plateaus for the alternating DNA copolymer. In addition, the plateau length and its mechanical stability match well with the expected values for each hairpin. This directly supported the conformation of tandemly arranged hairpins in the DNA homopolymer. When the unfolding force for the weaker hairpins is reached, these hairpins undergo collective unfolding, showing the low-force plateau, which is followed by a second, higher force plateau in which stronger hairpins start to unfold collectively.

To reveal the minimal number of DNA hairpins that start to show ensemble behaviors, we varied the number of hairpins contained inside a template. Individual transitions still occur when 2−9 hairpins are tandemly arranged in the template (Figure 1D). When more than 9 hairpins are incorporated in the template, individual folding/unfolding transitions start to disappear (Figures 1D & S13), suggesting that these hairpins start to show collective behaviors. The exact mechanism of the collective transition of all tandem hairpins is not clear. It is possible that due to the elastic property of the DNA strand, unfolding of one hairpin unit slightly reduces the tension in the template, which stabilizes the force in the plateau, acting like a force clamp. As the number of DNA hairpins in the homopolymer is increased ($n > 9$), there is dynamic unfolding and refolding of many hairpins in the DNA homopolymer simultaneously. The transition processes therefore appear to be indistinguishable among many hairpin units.

Ensemble Mechanochemical Sensing Using Single-Molecule DNA Homopolymers. Next, we evaluated the capability of tandem hairpins in the DNA homopolymer to detect analytes in single-molecule mechanochemical sensing (SMMS[12]). To this end, an 8 nt toehold[25] was placed at the 5′-end of each hairpin dispersed by a 24 nt spacer to recognize DNA targets using Watson-Crick base pairing (Figure 2A, states I&III). The toehold binding leads to full hybridization between the hairpin stem and the target DNA oligo (Table S3, oligo-23), which chemically unfolds the hairpin (state II) and induces a longer extension of the template. Using a standalone hairpin template, such single-molecule mechanochemical sensing has shown a detection limit of 5 nM for a DNA surrogate of Let-7a miRNA[26] (Figure S16) in 28 min.

In the following step, we investigated the binding of the same DNA surrogate to tandem hairpins in the DNA homopolymer. First, we collected F−X curves of the DNA homopolymer prepared by RCA (see Supporting Information and Experimental Section for details). The 9-pN transition plateau was clearly seen without a DNA target (Figure 2B, red trace), from which we determined the number of hairpins in each DNA homopolymer (see Supporting Information and Figure S6). We then transported tandem hairpins to the microfluidic channel that contained 1 fM to 1 μM DNA targets. At nanomolar concentrations (10 nM, Figure 2B), we observed the gradual shortening of the plateaus in minutes, indicating that chemical unfolding of hairpins by DNA targets was relatively slow at this concentration. When we plotted

https://dx.doi.org/10.1021/acs.analchem.0c02196
Anal. Chem. 2020, 92, 13126−13133

together F−X traces at different times, we found that below the plateau force, the extension of the template became longer over time, indicating the conversion of state I to state II (Figure 2A). However, above the plateau force, extension became shorter over time. At this high force, the hairpin was mechanically unfolded to give single-stranded DNA (state III). Upon hybridization with target DNA, the tandem-hairpin construct became shorter because of the duplex DNA formation (state IV), which has a shorter contour length than single-stranded DNA.[27] Strikingly, all the curves pass through an identical spot named the isoFX point, which is located at the cross point between the transition plateau and the curve in which all tandem hairpins are bound with DNA targets (Figure 2B). Similar to the isosbestic point in absorption spectroscopy,[28] the presence of the isoFX point indicates a process involving two inter-convertible species whose properties are linearly dependent on respective populations. In our case, many folded and unfolded hairpins in the DNA homopolymer convert into each other in a manner resembling the equilibrium process in bulk. This observation gives another support that tandem hairpins show ensemble behaviors.

At higher concentrations (1 μM), binding of DNA targets resulted in the disappearance of the plateau within 156 s (Figure S18A), indicating efficient unfolding of the hairpins in the tandem array (Figure 2A, states I → II → IV). To quantify the time constant of the target binding, we evaluated the number of folded hairpins versus total hairpins at a particular time when the tandem hairpins were incubated with the DNA target (see Figures S18B,C and S19). Assuming a pseudo first-order reaction of the binding,[16] fitting using a single-exponential function revealed a time constant of τ = 20 s for 1 μM (Figure S18C) and τ = 224 s for 10 nM DNA targets (Figure S18B). In general, the target binding kinetics increased with target concentrations (Figure S18D). Notably, binding rates remained small until the target concentration reached above 10 nM, at which a rapid increase in kinetics was observed. Such a behavior suggests a cooperative hybridization process between DNA targets and tandem hairpins in single-molecule DNA homopolymer templates.

After elucidating the interaction between DNA targets and tandem hairpins in the DNA homopolymer, we exploited these tandem DNA hairpins to detect miRNAs, a new set of biomarkers for many diseases.[29] We evaluated the binding of Let-7a miRNA[26] in the Tris buffer as well as in 10% serum to the DNA homopolymer with a similar number of hairpins (Figure 3, n = 174 ± 5 hairpins). Similar to the DNA surrogate, the plateau disappeared at high Let-7a concentrations whereas changes in extension were observed at low concentrations either below or above the plateau force (Figure 3A). After comparing these extension changes without and with Let-7a in Tris buffer (Figure 3B,C) or 10% serum (Figure 3D,E), we found the 1 fM limit of detection (for LOD see Figure S20 and Supporting Information for definition) in both media in 20 min. When we studied the effect of the number of hairpins on the detectability of the DNA homopolymer in the presence of 1 fM Let-7a within 20 min (Figure S21), we found that the number of the Let-7a-bound hairpin probes in the DNA homopolymer reached a maximum around 194 hairpins (Figure S21A). It is clear that when the number of hairpins increases, there is more chance for the analyte to bind. However, further increase in the hairpin number (beyond n = 194) leads to the coiling of the long DNA homopolymer because of entropic contributions. The coiling gives steric hindrance for the analyte to bind to the DNA homopolymer. When we plotted out the probe usage (percentage of the miRNA-bound hairpins) versus total hairpins (Figure S21B), we found that an increase in the number of hairpins reduced the probe usage. This is expected because most probes in ensemble sensing should not bind with targets when analytes are at low concentrations. Such a result indicated that single molecule sensing is rather efficient in the usage of the probe materials, which we describe as atom economy in sensing. Next, we evaluated the relationship between the binding percentage of the Let-7a to the DNA homopolymer (n = 167 ± 25 hairpins) under different miRNA concentrations within a 20 min sensing window. We found an exponential relationship (Figure S24), which can be used as a calibration curve to quantify the concentration of the miRNA in this single-molecule mechanochemical sensing method.

Compared to the sensing using standalone hairpins (LOD = 5 nM within 28 min, Figure S16), tandem hairpins in the DNA homopolymer (LOD = 1 fM within 20 min, Figure S20) decreased the detection limit by ∼6 orders of magnitude within 20 min. Such a low detection limit is superior to many miRNA detection methods[30] except RT-PCR, in which convoluted amplifications are required, which do not uniformly work among different miRNA species.[31] This striking improvement in the detection limit can be understood as follows. First, multiple hairpins in the DNA homopolymer increase the effective concentration of the sensing units, facilitating the binding of analytes within shorter time. Second, the close arrangement of hairpins allows rebinding of the analyte dissociated from the neighboring units. Finally, the pronounced ensemble behavior of transition plateau and the single-molecule sensitivity permit facile detection of signals associated with analyte binding. The detection limit can be further improved by adjusting the toehold length. By increasing toehold length from 8 to 11 nt, we found that the detection limit of standalone hairpins was improved by 4 orders of magnitude (Figure S17). Assuming this improvement persists in tandem hairpins, we anticipate that the detection limit may approach to the RT-PCR methods.

Single-Molecule Multiplex Sensing Using Alternating DNA Copolymers. To explore the possibility of multiplex sensing using ensemble behaviors of tandem hairpins, we prepared a DNA homopolymer that contains a tandem array of another DNA hairpin that can recognize miRNA 151 (mi151).[32] To differentiate the plateau force of the mi151 hairpin from that of the Let-7a hairpin (Figure 3), a 25 bp stem with higher GC content (68%) was used in this hairpin (Figure 4, see Table S3 for the sequence of the hairpin). Similar to the Let-7a sensing, the mi151 first binds to the 9 nt toehold outside the hairpin. It then invades until the 12th base (counted from the bottom of the hairpin) in the stem, leaving the upper 13 base pairs intact in the hairpin (Figure 4A) during the mechanical unfolding process. Because binding of the mi151 only partially disassembles the hairpin, the F−X curves showed a shortened force plateau at ≥10 nM miRNA (Figure 4B,C). Notably, the plateau became even shorter in the relaxing F−X curves, causing the hysteresis between stretching and relaxing F−X curves (see Figure S22 for the calculation of the hysteresis area). This can be ascribed to the slow refolding from the partially folded hairpins (Figure 4A, state II) to the fully folded hairpins (state I) because the bound mi151 needs to be displaced. Such a hysteresis can be used to indicate the

https://dx.doi.org/10.1021/acs.analchem.0c02196
Anal. Chem. 2020, 92, 13126−13133

binding of the mi151. Compared to the Let-7a sensing, the signal change observed for the mi151 binding was weaker, which led to a higher detection limit (10 nM for the mi151 in Figures 4&S23) compared to the Let-7a (1 fM, Figure 3C,E) in 20 min.

Because the GC content in the mi151 sensor (68%) is higher than the Let-7a sensor (43%), we observed a plateau of increased force for the former DNA homopolymer sensor (∼14−15 pN, Figure 4B,C) than the latter (∼9 pN, Figure 3). This difference was exploited in the multiplex sensing of both mi151 and Let-7a in the alternating DNA copolymer (Figure 5). Without targets, the multiplexing sensor showed two plateaus corresponding to the unfolding of two different hairpins, respectively (Figure 5B). In the presence of either 100 nM Let-7a (Figure 5C, pink trace) or 100 nM mi151 (Figure 5C, curves with cyan hysteresis), either the ∼9 pN plateau disappeared (Figure 5C, pink trace) or the ∼14−15 pN relaxing plateau became shortened (also demonstrated by the cyan hysteresis between the stretching and relaxing F−X curves, Figure 5C), indicating the binding of miRNA targets to the respective hairpin probes in the alternating DNA copolymer. It is interesting that a hysteresis was also observed for the lower plateau (∼9 pN) in the presence of the mi151 (Figure 5C, cyan hysteresis). This is again because of the slow refolding of the mi151-bound hairpins, which were not fully refolded even when the weaker hairpins for the Let-7a targeting started to reform. When both Let-7a (100 nM) and mi151 (100 nM) were present, the ∼9 pN plateau disappeared while the ∼14−15 pN relaxing plateau shortened with an expected hysteresis (Figure 5C, curves with green hysteresis), indicating the binding of both miRNAs. These results clearly demonstrated the multiplexing sensing capability of the single-molecule alternating DNA copolymers.

■ CONCLUSIONS

In summary, by evaluating up to hundreds of tandemly arranged hairpins in DNA homopolymers prepared by RCA, we found that as few as 10 tandem DNA hairpins in a single-molecule template showed ensemble behaviors. By exploiting these ensemble behaviors in the DNA homopolymers or alternating DNA copolymers, we developed new sensing strategies that combine the accuracy (concentration detection limit) in the ensemble sensing with the precision (mass detection limit) in the single-molecule sensing. Using DNA homopolymers, we were able to detect femtomolar miRNA in 10% serum in 20 min, an improvement of 6 orders of magnitude compared to standalone hairpin sensing. In addition, multiplex sensing of miRNA was achieved by incorporation of different hairpin probes in an alternating DNA copolymer. Given the versatility of many nucleic acid-based recognition elements, the simple RCA preparations, as well as the sensitivity and accuracy inherent in this ensemble single-molecule sensing, we expect that the new DNA copolymers described in this work can provide a wide range of applications in the biosensing, biophysics, and biomaterials fields.

■ ASSOCIATED CONTENT

Supporting Information

The Supporting Information is available free of charge at https://pubs.acs.org/doi/10.1021/acs.analchem.0c02196.

Preparation of DNA handles for syntheses of single- and double-hairpin constructs, synthesis of a double-hairpin construct, synthesis of the biotin primer for RCA, syntheses of DNA homopolymers and copolymers using RCA, four-channel microfluidic chamber, calculation of change-in-contour-length and number of hairpins in DNA constructs, force analyses of the DNA homopolymers versus standalone hairpins, unfolding force histogram of double-hairpins, effect of $MgCl_2$ on the transition plateau, predicted mfold structures with different repetitions of template unit, F−X traces of DNA homopolymers, fitting ssDNA construct using a freely jointed chain model, fitting ssDNA construct using a worm-like chain model, limit of detection for standalone hairpins, characterization of binding of target DNA to a tandem hairpin probe, temporal F−X curves of DNA homopolymers in the presence of target DNAs, limit of detection for DNA homopolymers, effect of the homopolymer length on the miRNA binding, binding of the mi151 to the DNA homopolymer with high GC content hairpins, calibration curve for Let-7a using DNA homopolymers, and sequences of oligonucleotides used in this study (PDF)

■ AUTHOR INFORMATION

Corresponding Author

Hanbin Mao − *Department of Chemistry & Biochemistry and School of Biomedical Sciences, Kent State University, Kent, Ohio 44242, United States;* orcid.org/0000-0002-6720-9429; Email: hmao@kent.edu

Authors

Sagun Jonchhe − *Department of Chemistry & Biochemistry and School of Biomedical Sciences, Kent State University, Kent, Ohio 44242, United States;* orcid.org/0000-0003-4361-6641

Sangeetha Selvam − *Department of Chemistry & Biochemistry and School of Biomedical Sciences, Kent State University, Kent, Ohio 44242, United States*

Deepak Karna − *Department of Chemistry & Biochemistry and School of Biomedical Sciences, Kent State University, Kent, Ohio 44242, United States;* orcid.org/0000-0003-3370-0997

Shankar Mandal − *Department of Chemistry & Biochemistry and School of Biomedical Sciences, Kent State University, Kent, Ohio 44242, United States;* orcid.org/0000-0002-2653-8760

Benjamin Wales-McGrath − *Department of Chemistry & Biochemistry and School of Biomedical Sciences, Kent State University, Kent, Ohio 44242, United States*

Complete contact information is available at: https://pubs.acs.org/10.1021/acs.analchem.0c02196

Notes

The authors declare no competing financial interest.

■ ACKNOWLEDGMENTS

H.M. thanks National Science Foundation [CHE-1609514 & CBET-1904921] for sensing experiments; National Institutes of Health [NIH 1R01CA236350] for DNA construct preparations.

REFERENCES

(1) Miles, B. N.; Ivanov, A. P.; Wilson, K. A.; Doğan, F.; Japrung, D.; Edel, J. B. *Chem. Soc. Rev.* **2013**, *42*, 15−28.
(2) Walt, D. R. *Anal. Chem.* **2013**, *85*, 1258−1263.
(3) Varongchayakul, N.; Song, J.; Meller, A.; Grinstaff, M. W. *Chem. Soc. Rev.* **2018**, *47*, 8512−8524.
(4) Labeit, S.; Kolmerer, B. *Science* **1995**, *270*, 293−296.
(5) Cimino-Reale, G.; Pascale, E.; Battiloro, E.; Starace, G.; Verna, R.; D'Ambrosio, E. *Nucleic Acids Res.* **2001**, *29*, No. e35.
(6) Doudna, J. A.; Charpentier, E. *Science* **2014**, *346*, 1258096.
(7) Cong, L.; Ran, F. A.; Cox, D.; Lin, S.; Barretto, R.; Habib, N.; Hsu, P. D.; Wu, X.; Jiang, W.; Marraffini, L. A.; Zhang, F. *Science* **2013**, *339*, 819−823.
(8) Nam, K. H.; Haitjema, C.; Liu, X.; Ding, F.; Wang, H.; DeLisa, M. P.; Ke, A. *Structure* **2012**, *20*, 1574−1584.
(9) Fire, A.; Xu, S. Q. *Proc. Natl. Acad. Sci. U.S.A.* **1995**, *92*, 4641−4645.
(10) Liu, D.; Daubendiek, S. L.; Zillman, M. A.; Ryan, K.; Kool, E. T. *J. Am. Chem. Soc.* **1996**, *118*, 1587−1594.
(11) Li, Q.; Zhao, J.; Liu, L.; Jonchhe, S.; Rizzuto, F. J.; Mandal, S.; He, H.; Wei, S.; Sleiman, H. F.; Mao, H.; Mao, C. *Nat. Mater.* **2020**, *19*, 1012.
(12) Koirala, D.; Shrestha, P.; Emura, T.; Hidaka, K.; Mandal, S.; Endo, M.; Sugiyama, H.; Mao, H. *Angew. Chem., Int. Ed. Engl.* **2014**, *53*, 8137−8141.
(13) Mao, H.; Luchette, P. *Sens. Actuators, B* **2008**, *129*, 764−771.
(14) Woodside, M. T.; Anthony, P. C.; Behnke-Parks, W. M.; Larizadeh, K.; Herschlag, D.; Block, S. M. *Science* **2006**, *314*, 1001−1004.
(15) Onoa, B.; Dumont, S.; Liphardt, J.; Smith, S. B.; Tinoco, I., Jr.; Bustamante, C. *Science* **2003**, *299*, 1892−1895.
(16) Koirala, D.; Dhakal, S.; Ashbridge, B.; Sannohe, Y.; Rodriguez, R.; Sugiyama, H.; Balasubramanian, S.; Mao, H. *Nat. Chem.* **2011**, *3*, 782−787.
(17) Rief, M.; Oesterhelt, F.; Heymann, B.; Gaub, H. E. *Science* **1997**, *275*, 1295−1297.
(18) Neupane, K.; Foster, D. A. N.; Dee, D. R.; Yu, H.; Wang, F.; Woodside, M. T. *Science* **2016**, *352*, 239−242.
(19) Woodside, M. T.; Behnke-Parks, W. M.; Larizadeh, K.; Travers, K.; Herschlag, D.; Block, S. M. *Proc. Natl. Acad. Sci. U.S.A.* **2006**, *103*, 6190−6195.
(20) Zimm, B. H.; Bret, M. L. *J. Biomol. Struct. Dyn.* **1983**, *1*, 461−471.
(21) Manning, G. S. *J. Chem. Phys.* **1969**, *51*, 924−933.
(22) Anderson, C. F.; Record, M. T. *Annu. Rev. Phys. Chem.* **1982**, *33*, 191−222.
(23) Špringer, T.; Šípová, H.; Vaisocherová, H.; Štěpánek, J.; Homola, J. *Nucleic Acids Res.* **2010**, *38*, 7343−7351.
(24) McIntosh, D. B.; Saleh, O. A. *Macromolecules* **2011**, *44*, 2328−2333.
(25) Zhang, D. Y.; Winfree, E. *J. Am. Chem. Soc.* **2009**, *131*, 17303−17314.
(26) Takamizawa, J.; Konishi, H.; Yanagisawa, K.; Tomida, S.; Osada, H.; Endoh, H.; Harano, T.; Yatabe, Y.; Nagino, M.; Nimura, Y.; Mitsudomi, T.; Takahashi, T. *Cancer Res.* **2004**, *64*, 3753−3756.
(27) Voet, D.; Voet, J. G. *Biochemistry*, 2nd ed.; John Wiley and Sons, Inc.: New York, 1995.
(28) Harris, D. C. *Quantitative Chemical Analysis*, 8th ed.; W. H. Freeman and Company: New York, 2010.
(29) Chen, X.; Ba, Y.; Ma, L.; Cai, X.; Yin, Y.; Wang, K.; Guo, J.; Zhang, Y.; Chen, J.; Guo, X.; Li, Q.; Li, X.; Wang, W.; Zhang, Y.; Wang, J.; Jiang, X.; Xiang, Y.; Xu, C.; Zheng, P.; Zhang, J.; Li, R.; Zhang, H.; Shang, X.; Gong, T.; Ning, G.; Wang, J.; Zen, K.; Zhang, J.; Zhang, C.-Y. *Cell Res.* **2008**, *18*, 997−1006.
(30) Li, W.; Ruan, K. *Anal. Bioanal. Chem.* **2009**, *394*, 1117−1124.
(31) Chim, S. S. C.; Shing, T. K. F.; Hung, E. C. W.; Leung, T.-y.; Lau, T.-k.; Chiu, R. W. K.; Dennis Lo, Y. M. *Clin. Chem.* **2008**, *54*, 482−490.
(32) Oved, K.; Morag, A.; Pasmanik-Chor, M.; Oron-Karni, V.; Shomron, N.; Rehavi, M.; Stingl, J. C.; Gurwitz, D. *Pharmacogenomics* **2012**, *13*, 1129−1139.

https://dx.doi.org/10.1021/acs.analchem.0c02196
Anal. Chem. 2020, 92, 13126−13133